2019 Chinese Control Conference

Proceedings of the 38th CCC

第三十八届中国控制会议论文集

Technical Committee on Control Theory

English

前言

会议机构

报告人介绍

关肇直奖

张贴论文奖

论文目录

全文搜索

作者索引

主办单位：中国自动化学会控制理论专业委员会
中国自动化学会
中国系统工程学会

承办单位：广东工业大学

协办单位：中国科学院数学与系统科学研究院
中国工业与应用数学学会
华南理工大学
广东省自动化学会
亚洲控制学会
IEEE控制系统协会
韩国控制、机器人与系统学会
日本仪器与控制工程师学会

IEEE Catalog Number: CFP1940A-USB
ISBN: 978-988-15639-6-5
ISBN 978-988156396-5

2019年7月27-30日　　中国·广州

Proceedings of the 38th Chinese Control Conference
July 27-30, 2019, Guangzhou, China

A Fast-Online Guidance Method for Trajectory Correction Projectiles

Yuhan Mou[1], Jing Zhang[1], Lingyu Yang[1], Xiaoke Feng[1]

1. School of Automation Science and Electrical Engineering, Beihang University, Beijing 100191
E-mail: mouyh@buaa.edu.cn, zhangjing2013@buaa.edu.cn, yanglingyu@buaa.edu.cn, 18580530093@163.com

Abstract: The fast-online guidance problem of trajectory correction projectile is investigated in this paper. The dynamic mathematical model of spin-stability projectile is briefly presented and a simplified process for the nonlinear seven degree of freedom model is given in detail. Then a linear approximate model is introduced to calculate trim points along the projectile trajectory, and the trajectory characteristics is given through the trim results. A real-time method for calculating the control angle of the course correction fuse is also proposed base on the above trim method. Finally, simulation results are given to validate the proposed method.

Key Words: Course correction fuse, trajectory correction, flight control, spin-stability projectile

Nomenclature

δ_1, δ_2	Angle of attack, Angle of sideslip
φ_a, φ_2	Euler pitch and yaw angles
θ_a, ψ_2	Flight-path angles
γ_c	Control roll angle
m, g	Mass, gravitational accelerate
$\omega_\eta, \omega_\zeta$	Pitch and yaw rates
$\omega_{f\xi}, \omega_{a\xi}$,	Roll rates of the head and rear
C_a, A	Moment of inertial about the axis frame ξ and η axes
S, l, d	Reference area, length and diameter of projectile
$C_D, C_{L\delta_r}$	Drag and lift coefficients
$C_{M\delta_r}, C_{Mq}$	Static moment and damping moment coefficients
$C_{Mp\delta_r}$	Magnus moment coefficients
$C_{L\delta_c}, C_{M\delta_c}$	Lift and static moment coefficients of the canards
X, Y, Z	Positon vector components of the composite center of mass
v_r	Magnitude of airspeed
$\boldsymbol{\omega_T}, \boldsymbol{\omega_A}$	Angular rates vectors of the trajectory and axis frame with the respect to base frame

1 Introduction

The requirements on high deliver accuracy and long range of modern weapons are increasingly strict with the development of the war. The poor accuracy of the unguided shells could reduce the efficiency of combat and even leads to damage on friendly sides. Thus, it is necessary to modify the existing shells to improve its performance and remain inexpensive meanwhile. Course Correction Fuse (CCF) is an effective approach to transform the existing unguided shells to smart ammunitions. An unguided projectile of howitzer or mortar could become a Trajectory Correction Projectile (TCP) after simply replace its fuse by CCF. The CCF concept is illustrated in Fig. 1. Two pairs of canards are installed in the CCF. The canards 1-3 are installed in opposed angle to provide control force $\boldsymbol{F_c}$ while the canards 2-4 are installed in same angle to provide axial moment. Control roll angle γ_c is used to describe the direction of $\boldsymbol{F_c}$.

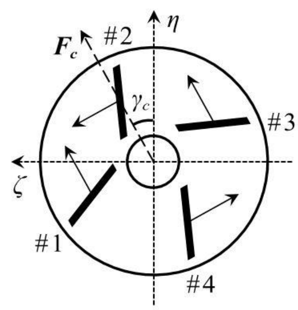

Fig. 1: Concept of the course correction fuse

The CCF considered in this paper is used in the 155mm howitzer which maintains the stability by the gyroscopic effect, i.e., a spin-stability projectile. Thus, a structure called dual-spin projectile is considered in the design. Dual-spin projectile includes two parts, the head part and the rear part, as shown in the Fig. 2. Motor and Bearings are used to despin the canards attached to the head part and keep $\boldsymbol{F_c}$ in the designated direction, while the rear is keep a high spin rate to maintain the stability.

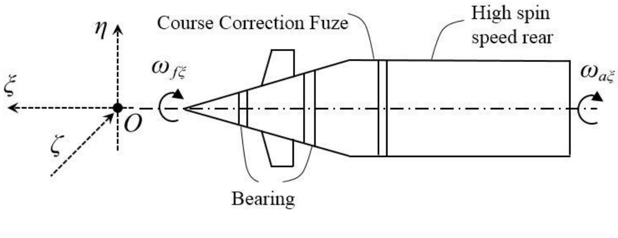

Fig. 2: Dual-spin projectile structure

The modelling of the TCP are widely studied. An important feature of the TCP model is that it has an extra degree of freedom (DOF) compared to common projectiles. Nicolas [1] study the problem of aerodynamics of TCP by calculation fluid dynamic (CFD) methods. Eric [2,3] acquires the aerodynamic parameter through the software Missile DTACOM. Dr. Cheng [4] builds the mathematical model of TCP based on CFD and experiment comprehensively, which laid the foundation of simulation and analysis.

The canards 1-3 are fixed on the CCF, so the γ_c control both the vertical and lateral sides of the trajectory correction simultaneous, which causes serious couple in the vertical and lateral moments. More complicatedly, due to the unique dynamic characteristic of the spin-stability projectile, the direction of control load lags in phases with the γ_c. Above features make it hard to solve the γ_c accurately when a designated direction of load is needed. Seve Florian [5] simplified the 6 DOF model of shell based on the stability assumption and studies the flight characteristic. Philippe Wernert [6] and Spilios Theodoulis [7] provide another method to simplify the model of TCP and calculate trim point of the projectile. Although the CCF considered in this paper is different from theirs, the similar method is adopted in this paper. Dr. Cheng [4] points that there is an approximate phase lag π between γ_c and direction of load. Nevertheless the systematic error exist in this method as the system is time varying.

A novel method based on the simplified model to solve γ_c is proposed in this paper, and the calculation is simplified to run online of the CCF.

The article is organized as follows. Section 1 introduce the background of the research. Section 2 builds the 7 DOF model of the TCP and given the simplified model. Section 3 details the methods to solve γ_c. Section 4 gives the simulation results, and the conclusion is drawn in section 5.

2 TCP modelling and simplify

Three coordinate systems (CS) are introduced [8] as follows: axis CS $O_{A-\xi\eta\zeta}$, base CS O_{N-xyz}, and trajectory CS $O_{T-x_2y_2z_2}$. φ_2, φ_a are defined to transform the base CS into axial CS. ψ_2, θ_a are defined to transform the base CS into trajectory CS. δ_2, δ_1 are defined to transform the trajectory CS into axial CS.

According to momentum theorem and moment of momentum theorem, the kinetic equations is given as Eq.(1).

$$\begin{cases} m\dfrac{\mathrm{d}\boldsymbol{v}}{\mathrm{d}t} = m\dfrac{\partial \boldsymbol{G}}{\partial t} + m\boldsymbol{\omega_T}\times\boldsymbol{v} = \boldsymbol{F_T} \\ \dfrac{\mathrm{d}\boldsymbol{G}}{\mathrm{d}t} = \dfrac{\partial \boldsymbol{G}}{\partial t} + \boldsymbol{\omega_A}\times\boldsymbol{G} = \boldsymbol{M_A} \end{cases}, \tag{1}$$

where $\boldsymbol{v}$ denotes the speed vector, $\boldsymbol{G}$ denotes momentum moment vector, and the aerodynamic coefficients used to calculate $\boldsymbol{F_T}$ and $\boldsymbol{M_A}$ are obtained with CFD methods. The angle δ_c is defined to describe the air speed with respect to the canards as the canards despin with the rear of projectile. The 7 DOF model of the TCP can be built with the kinetic equations (1) and geometric Eq. (2).

$$\begin{cases} \sin\delta_2 = \cos\psi_2\sin\varphi_2 - \sin\psi_2\cos\varphi_2\cos(\varphi_a - \theta_a) \\ \sin\delta_1 = \cos\varphi_2\sin(\varphi_a - \theta_a)/\cos\delta_2 \\ \sin\delta_c = \sin\delta_1\cos\gamma_c + \sin\delta_2\cos\delta_1\sin\gamma_c \end{cases} \tag{2}$$

Spilios Theodoulis [7] states that the spin-stability projectile experiences two major phenomena include precession and nutation. Precession denotes the low frequency motions and nutation denotes the higher ones. Without loss of generality, we select the lower frequency motion states $[v_r, \omega_{a\xi}, \varphi_2, Y]^T$ as the parameter vector $\boldsymbol{\rho}$, the higher frequency motion states $[\delta_1, \delta_2, \omega_\eta, \omega_\zeta]^T$ as the state vector $\boldsymbol{x}$, the acceleration $[a_\eta, a_\zeta]^T$ in axis CS as the output vector $\boldsymbol{y}$. Then we could acquire the four-order dynamic Eq. (3).

$$\begin{cases} \dfrac{\mathrm{d}\delta_1}{\mathrm{d}t} = \dfrac{g}{v_r}\cos\varphi_a - \dfrac{qS}{v_r m}[C_D\delta_1 + C_{L\delta_r}\delta_1 + C_{L\delta_c}(\delta+\delta_c)\cos\gamma_c] + (\omega_\zeta + \omega_\zeta\tan\varphi_2\delta_2) \\ \dfrac{\mathrm{d}\delta_2}{\mathrm{d}t} = -\dfrac{qS}{v_r m}[C_D\delta_2 + C_{L\delta_r}\delta_2 + C_{L\delta_c}(\delta+\delta_c)\sin\gamma_c] + (-\omega_\eta + \omega_\zeta\tan\varphi_2\delta_1) \\ \dfrac{\mathrm{d}\omega_\eta}{\mathrm{d}t} = \dfrac{qSl}{A}\left[-C_{M\delta_r}\delta_2 - \dfrac{d}{v_r}C_{Mq}\omega_\eta + \dfrac{d}{v_r}C_{Mp\delta_r}\omega_{a\xi}\delta_1 - C_{M\delta_c}(\delta+\delta_c)\sin\gamma_c\right] - \dfrac{C_a}{A}\omega_{a\xi}\omega_\zeta + \omega_\zeta\omega_\zeta\tan\varphi_2 \\ \dfrac{\mathrm{d}\omega_\zeta}{\mathrm{d}t} = \dfrac{qSl}{A}\left[C_{M\delta_r}\delta_1 - \dfrac{d}{v_r}C_{Mq}\omega_\zeta + \dfrac{d}{v_r}C_{Mp\delta_r}\omega_{a\xi}\delta_2 + C_{M\delta_c}(\delta+\delta_c)\cos\gamma_c\right] + \dfrac{C_a}{A}\omega_{a\xi}\omega_\eta - \omega_\eta\omega_\zeta\tan\varphi_2 \end{cases}, \tag{3}$$

where $q = \dfrac{\rho {v_r}^2}{2}$ denotes dynamic pressure.

The nonlinear system reach stable states when condition $\left[\dfrac{\mathrm{d}\delta_1}{\mathrm{d}t}, \dfrac{\mathrm{d}\delta_2}{\mathrm{d}t}, \dfrac{\mathrm{d}\omega_\eta}{\mathrm{d}t}, \dfrac{\mathrm{d}\omega_\zeta}{\mathrm{d}t}\right]^T = \boldsymbol{0}$ is satisfied, i.e. the state $\boldsymbol{x}$ which regards as the trim point could denotes the lower-frequency motion approximately. The nonlinear equations (3) can be solved by fix-point iteration method. Nevertheless, this method is not proper to run online on the CCF for its complexity.

A solution process to solve trim point is proposed based on linear equations in this paper, and the linear equations are acquired by simplifying the nonlinear Eq. (3). δ_1, δ_2, φ_2, ψ_2, $\varphi_a - \theta_a$, $\omega_\zeta\omega_\zeta\tan\varphi_2$ and $\omega_\eta\omega_\zeta\tan\varphi_2$ can regard as small quantities [8] for a normal trajectory, and the assumptions $\delta_1 \approx \varphi_a - \theta_a$, $\delta_2 \approx \varphi_2 - \psi_2$ also stand. Ignore the higher order item in (3) and let $\dot{\boldsymbol{x}} = \boldsymbol{0}$, then we can acquire the linear equation $\boldsymbol{Px} = \boldsymbol{b}$ and solve the trim point through $\boldsymbol{x} = \boldsymbol{P}^{-1}\boldsymbol{b}$. The analytical formats of $\boldsymbol{P}$ and $\boldsymbol{b}$ are as Eq. (4) and Eq. (5).

$$\boldsymbol{P}=\begin{pmatrix} -k_v(C_D+C_{L\delta_r}+C_{L\delta_c}\cos^2\gamma_c) & -k_vC_{L\delta_c}\sin\gamma_c\cos\gamma_c & 0 & 1 \\ -k_vC_{L\delta_c}\cos\gamma_c\sin\gamma_c & -k_v(C_D+C_{L\delta_r}+C_{L\delta_c}\sin^2\gamma_c) & 1 & 0 \\ k_a\left(\dfrac{d}{v_r}C_{Mp\delta_r}\omega_{a\xi}-C_{M\delta_c}\cos\gamma_c\sin\gamma_c\right) & k_a(-C_{M\delta_r}-C_{M\delta_c}\sin^2\gamma_c) & k_a\left(-\dfrac{d}{v_r}C_{Mq}\right) & -\dfrac{C_a}{A}\omega_{a\xi} \\ k_a(C_{M\delta_r}+C_{M\delta_c}\cos^2\gamma_c) & k_a\left(\dfrac{d}{v_r}C_{Mp\delta_r}\omega_{a\xi}+C_{M\delta_c}\cos\gamma_c\sin\gamma_c\right) & \dfrac{C_a}{A}\omega_{a\xi} & k_a\left(-\dfrac{d}{v_r}C_{Mq}\right) \end{pmatrix}, \quad (4)$$

$$\boldsymbol{b}=\left(-\frac{g}{v_r}\cos\varphi_a+k_vC_{L\delta_c}\delta\cos\gamma_c \quad k_vC_{L\delta_c}\delta\sin\gamma_c \quad k_aC_{M\delta_c}\delta\sin\gamma_c \quad -k_aC_{M\delta_c}\delta\cos\gamma_c\right), \quad (5)$$

where $k_v=\dfrac{qS}{v_rm}$, $k_a=\dfrac{qSl}{A}$.

The output equations are given in Eq. (6).

$$\begin{cases} a_\eta=\dfrac{qS}{m}[C_D\delta_1+C_{L\delta_r}\delta_1+C_{L\delta_c}(\delta+\delta_c)\cos\gamma_c] \\ a_\zeta=\dfrac{qS}{m}[C_D\delta_2+C_{L\delta_r}\delta_2+C_{L\delta_c}(\delta+\delta_c)\sin\gamma_c] \end{cases} \quad (6)$$

Select the parameter vector $\boldsymbol{\rho}$ from a typical trajectory of 155mm howitzer at 80s, then we can acquire trim points though either linear simplified calculation method (LSCM) or nonlinear fix-point iteration method (NFPIM). The comparison of the results by two methods are shown as Figs. 3-6.

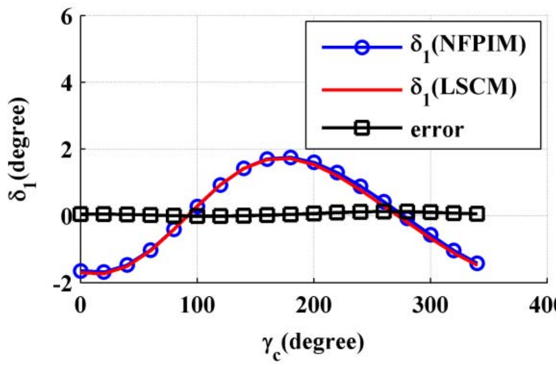

Fig. 3: Angle of attack at trim points

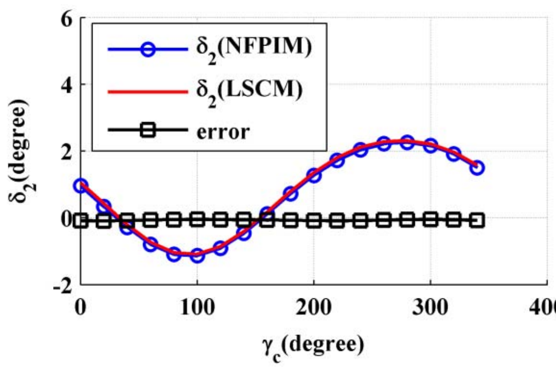

Fig. 4: Angle of sideslip at trim points

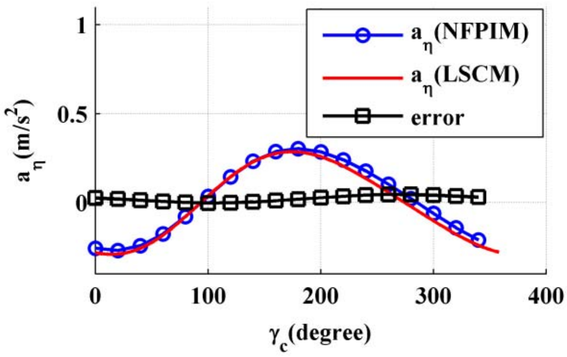

Fig. 5: Vertical acceleration at trim points

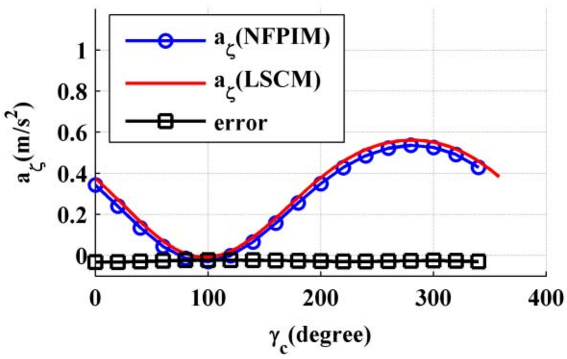

Fig. 6: Lateral acceleration at trim points

The root mean square error (RMSE) of LSCM is shown in Table 1. It can be seen from Figs. 3-6 and Table 1 that the computational complexity can be reduced by the LSCM with the guarantee of accuracy.

Table 1: RMSE of trim points by LSCM

Item	δ_1	δ_2	a_η	a_ζ
RMSE	$0.074°$	$0.071°$	$0.03\,m/s^2$	$0.03\,m/s^2$

The effect of the CCF on trajectory can be analyzed from the trim results. It can be seen from Fig. 6 that the maximum value of lateral accelerate on the opposite side of the axis ζ is close to zero under the control of canards at 80s. That means origin AOS exists in trajectory of the unguided shell due to the magnus and gyroscopic effects. Thus, the CCF can only correct the origin lateral shifting at 80s and the trim results cannot use for trajectory correction directly.

3 Impact correction with trim point

After we obtain trim points according to different γ_c by LSCM, the reflection from γ_c to the direction of load can be simply gotten in the trajectory. Nevertheless, the response load cannot represent the effect of CCF as the origin AOS always exists.

Without loss of generality, we can suppose that the load caused only by CCF add to the origin lateral load of unguided shell linearly. Then we have $\Delta a = a_c - a_0$, where Δa denotes the acceleration caused by CCF, a_c denotes the acceleration at trim point, a_0 denotes the origin acceleration. The a_0 can be obtained by letting the aerodynamic coefficients of canards, $C_{L\delta_c}$ and $C_{M\delta_c}$, equal to zero. Then the Δa on axis η and axis ζ can be solved by LSCM, and the results are shown in Figs .7-8.

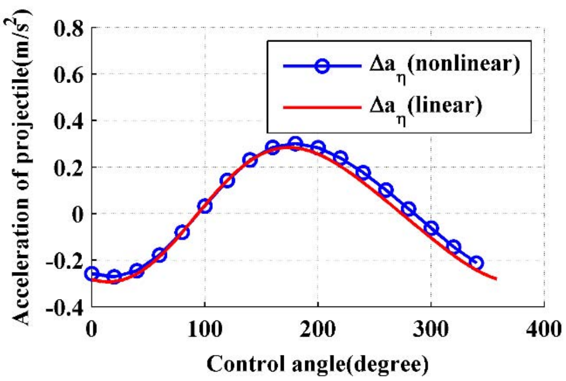

Fig. 7: Vertical acceleration of control canard

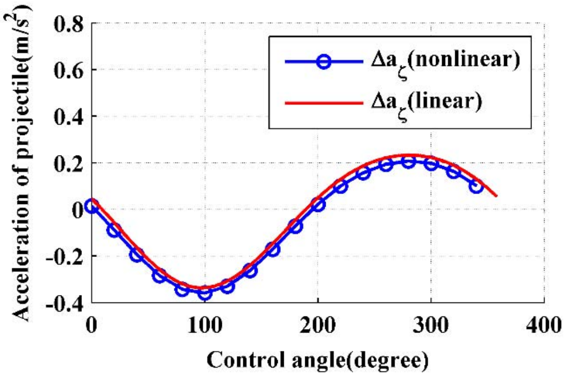

Fig. 8: Lateral acceleration of control canard

Define the orientation angle of the load caused by CCF as $\varepsilon = \mathrm{atan2}(\Delta a_\eta, \Delta a_\zeta)$, then the reflection from γ_c to ε can be calculated as Fig. 9-10. It can be seen that the reflection are approximately linear and an approximate phase lag π between γ_c and ε can be assumed. Then a more accurate method to calculate the γ_c can be further studied.

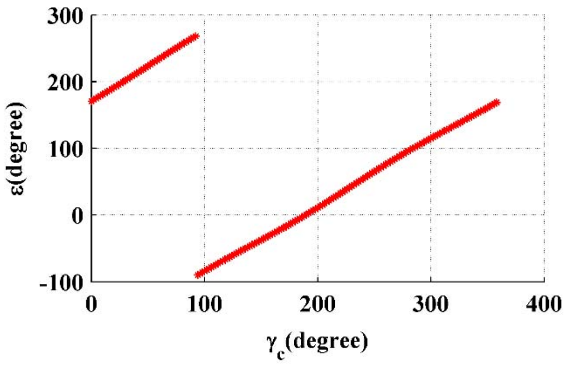

Fig. 9: Reflection from γ_c to ε

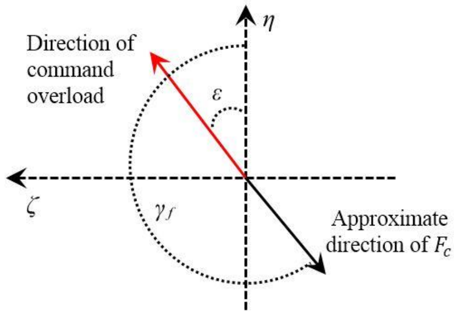

Fig. 10: The approximate relationship between the load and control force

The vertical load Δa_η can be decomposed into Δa_{x2} and Δa_{y2} in trajectory CS, which both have an influence on the range of TCP. The positive Δa_{y2} or Δa_{x2} can increase the range in terminal guidance section and vice versa. Thus, we have the assumption $\Delta a_\zeta \approx \Delta a_z$, $\Delta a_\eta \approx \Delta a_x$. Nevertheless, this assumption does not stand in the ascent trajectory.

CCF need to provide control load in designated direction according to the guidance law, which requires corresponding γ_c being calculated online on the CCF. As is states above, there is an approximately linear reflection from γ_c to ε, so it is reasonable to calculate some particular trim points in the neighborhood of possible orientation and use linear fitting to solve the reflection online.

An possible value of control roll angle γ_{cp} which is corresponding the command angle ε can be calculated by $\gamma_{cp} = \varepsilon + \pi$ because of the approximate phase lag. Then select $\gamma_{ci} = \gamma_{cp} \pm i\pi/18 \ (i = 0, 1, 2)$ and the corresponding ε_i can be solve by LSCM, respectively. It is supposed that a linear reflection $\hat{\gamma}_c = \hat{k}\varepsilon + b$ exists from ε to γ_c. A least square fitting is used here and the parameters $\hat{k}$, b can be solved in (7).

$$\begin{cases} \hat{k} = \dfrac{\sum_{i=1}^{5} \varepsilon_i \gamma_{ci} - \frac{1}{5}\sum_{i=1}^{5} \varepsilon_i \sum_{i=1}^{5} \gamma_{ci}}{\sum_{i=1}^{5} {\varepsilon_i}^2 - \frac{1}{5}\left(\sum_{i=1}^{5} \varepsilon_i\right)^2} \\ b = \hat{\gamma}_c - \hat{k}\varepsilon \end{cases} \tag{7}$$

It can be validated by the following simulation that the real time fitting calculation method (RTFCM) can obtain a more accurate impact correction than the approximate phase lag method (APLM).

4 Simulation Results

4.1 Initial condition of simulation

A 155mm shell model equipped with CCF is used in the simulation and its aerodynamic coefficients are acquired by CFD methods. The initial conditions are in Table 2.

Table 2: Initial conditions of the simulation

Item	value
velocity	980m/s
elevation	51°
azimuth	0°
rotation rate	1885rad/s
mass	45kg
polar moment of inertia	$0.16\mathrm{kg}\cdot\mathrm{m}^2$
altitude	0m
equatorial moment of inertia	$1.8\mathrm{kg}\cdot\mathrm{m}^2$

4.2 Verification of the trim point

The axis ξ of the projectile oscillates around the equilibrium axis because of the gyroscope effect of the spin-stability projectile, i.e., the nutation process. A comparison on the airflow angle between 7 DOF model and trim points by LSCM is made to validate the correctness of the simplified trim point. A fixed control $\gamma_c = 0$ is given to the model at 15s, and the results are shown in Figs. 11-12.

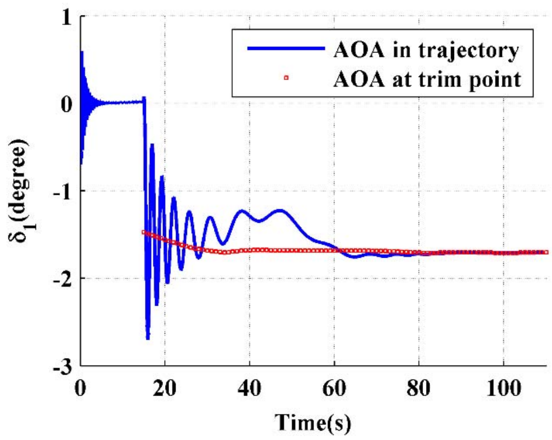

Fig. 11: Compassion between trim point and true value of AOA

It can be seen in the Fig. 11-12 that the trim points reflect the procession progress of the spin-stability projectile, especially in the terminal guidance section. This result provides a theoretical basis for control and guidance.

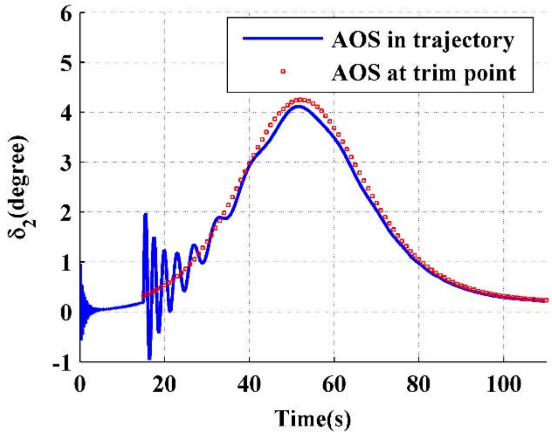

Fig. 12: Compassion between trim point and true value of AOS

4.3 Simulation for impact correction

An open-loop guidance is used to correct the impact of TCP in this scenario. The position of the impact can be controlled with the base of assumption $\Delta a_\zeta \approx \Delta a_z$, $\Delta a_\eta \approx \Delta a_x$ in the terminal guidance section. Define the orientation angle of impact as $\lambda = \mathrm{atan}2(\Delta Z, \Delta X)$, i.e., λ denotes the location of guided shell in relation to the unguided trajectory. The control of TCP starts at 50s after the apogee of trajectory, and a fixed ε value is given in the simulation. We finally acquire eight typical trajectories as we let $\lambda = n\pi/4$, where $n = 1, 2, ..., 8$.

Fig.13-14 show parts of the simulation results and $\lambda = 41°$, $-47°$ under the commands $\lambda_c = 45°$, $-45°$, respectively. Other results are listed in the Table 3 and the APLM is used as contrast. The RMSE and absolute error (AE) are also calculated in the simulation.

It can be seen from Table 3 and Table 4 that the γ_c calculated by RTFCM obtains more accurate results than the contrast in impact control. In addition, the parameter needed for RTFCM include air speed, rotation rate and position can be obtained from the GPS directly, thus the method is suitable to apply in engineering.

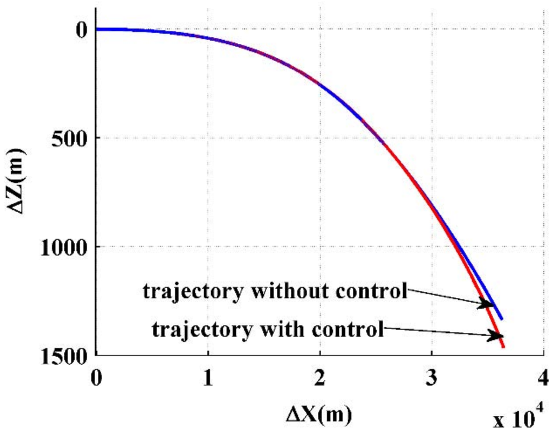

Fig. 13: Top view of the trajectory with the command 45°

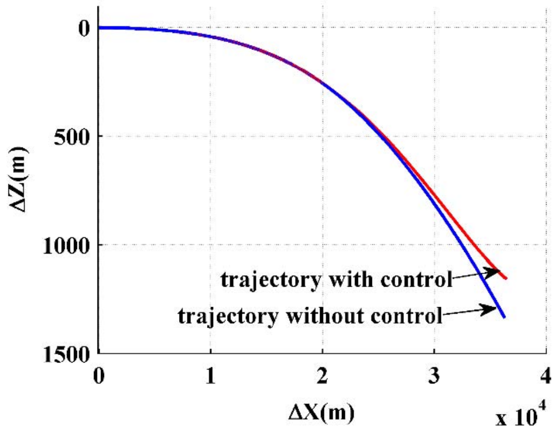

Fig. 14: Top view of the trajectory with the command $-45°$

Table 3: Control results of the λ

Command	RTFCM	AE	APLM	AE
0°	1°	1°	−4°	4°
45°	41°	4°	38°	7°
90°	78°	12°	76°	14°
135°	122°	13°	114°	21°
180°	169°	11°	156°	24°
225°	217°	8°	205°	20°
270°	264°	6°	258°	12°
315°	314°	1°	308°	7°

Table 4: RMSE of the simulation results

Method	RTFCM	APLM
RMSE	8.88°	16.56°

5 Conclusion

Based on the simplified linear model of TCP, this paper proposes the RTFCM to calculate the γ_c according to the command loads. Thus, the designated direction of the control load can be provided by canards with the effect of the high spin rate of howitzer. The RTFCM uses parameters which can be obtained from sensors and costs little computation time, i.e., it is suitable for online calculation. Future work will involve the research of the guidance law such as proportion navigation or impact prediction for the TCP, then the close-loop control can be realized on the TCP.

References

[1] Hamel N, Gagnon E. CFD and Parametric study on a 155 mm artillery shell equipped with a roll-decoupled course correction fuze[C]// Aiaa Applied Aerodynamics Conference. 2013.D. Cheng, Controllability of switched bilinear systems, *IEEE Trans. on Automatic Control*, 50(4): 511–515, 2005.

[2] Gagnon E, Lauzon M. Maneuverability Analysis of the Conventional 155 mm Gunnery Projectile[C]// AIAA Guidance, Navigation and Control Conference and Exhibit. 2006.H. Poor, *An Introduction to Signal Detection and Estimation*. New York: Springer-Verlag, 1985, chapter 4.

[3] Gagnon E, Lauzon M. Course Correction Fuze Concept Analysis for In-Service 155 mm Spin-Stabilized Gunnery Projectiles[C]// *AIAA Guidance, Navigation and Control Conference and Exhibit.* 2013.

[4] Cheng Jie. Flight Performance and Reduced Order Model of a Trajectory Correction Projectile with Decoupled Canards: [D]. Nanjing : Nanjing University of Science and Technology, 2016. (In Chinese)

[5] Seve F, Theodoulis S, Wernert P, et al. Flight Dynamics Modeling of Dual-Spin Guided Projectiles[J]. *IEEE Transactions on Aerospace & Electronic Systems,* 2017, PP(99):1-1.

[6] Wernert P, Theodoulis S. Modelling and Stability Analysis for a Class of 155 mm Spin-stabilized Projectiles with Course Correction Fuse (CCF)[C]// *AIAA Atmospheric Flight Mechanics Conference.* 2013.

[7] Theodoulis S, Gassmann V, Wernert P, et al. Guidance and Control Design for a Class of Spin-Stabilized Fin-Controlled Projectiles[J]. *Journal of Guidance Control & Dynamics*, 2013, 36(2):517-531.

[8] Han Zipeng, Exterior Ballistics of Projectiles and Rockets. Beijing, China: Beijing Institute of Technology Press, 2014, pp. 138-148.(In Chinses).